Fasudil attenuates Neuro-Inflammation and Oxidative Stress via Rhoa/Rock Pathways in Delayed Neuropsychologic Sequelae Mice Model

Xiang Yan
The Affiliated Hospital of Southwest Medical University
Meng Fu
The Affiliated Hospital of Southwest Medical University
Ye Gao
The Affiliated Hospital of Southwest Medical University
Qin Han
The Affiliated Hospital of Southwest Medical University
Shuang Li
The Affiliated Hospital of Southwest Medical University
Huan Xia
The Affiliated Hospital of Southwest Medical University
Jinglun Li (ljl0310611@163.com)
The Affiliated Hospital of Southwest Medical University

Research Article

Keywords: delayed neuropsychologic sequelae, carbon monoxide poisoning, oxidative stress, Fasudil, RhoA/ROCK pathway.

Posted Date: November 17th, 2021

DOI: https://doi.org/10.21203/rs.3.rs-1055014/v1

Abstract

Background

Delayed neuropsychologic sequelae is common in patients after carbon monoxide poisoning without effective methods worldwide. Fasudil exerts neuroprotective effect and alleviates oxidative stress in some neurodegenerative disorders. However, the mechanism between DNS and FS remains unclear. The study aims to explore the efficacy and mechanism of Fasudil in DNS mice model.

Objective

The delayed neuropsychologic sequelae model was induced with a hyperbaric oxygen chamber. All rats were randomly assigned to three groups (n=10): air control group (AC), CO poisoning group (CO), and CO poisoning +Fasudil group (CO+FS). Rats in the CO+FS group were given Fasudil (10 mg/kg/day, ip). The morris water maze was documented to estimate spatial learning and memory of mice. The demyelination state in brain was observed through LFB staining. The protein of MBP was examined with immunofluorescence staining. The levels of IL-6, TNF-α, TGF-β, SOD, and MDA were examined by ELISA. The mRNA levels of Rho, ROCK2, MLC1 and MYPT1 were analyzed by rt-PCR.

Result

The cognitive impairment in the CO+FS group were significantly reduced than those of the CO group ($P<0.05$). LFB staining and immunofluorescence staining of MBP results showed that FS significantly treatment attenuated demyelination ($P<0.05$). Compared with the CO group, the levels of TNF-α, IL-6, MDA, ROCK2, MLC1, and MYPT1 significantly decreased ($P<0.05$), and the levels of SOD were significantly increased in the CO+FS group ($P<0.05$).

Conclusion

In a word, Fasudil attenuated delayed neuropsychologic sequelae by inhibiting inflammation, oxidative stress and downregulating Rho/ROCK pathway in DNS mice model. We conclude that Fasudil may be a novel treatment for delayed neuropsychologic sequelae.

Background

Acute CO poisoning is one of the common and fatal cause of poisoning and its manifestations include mild headache, nausea, fatigue, dizziness, syncope, coma, seizures and even respiratory and circulatory failure and death[1]. DNS, also known as delayed encephalopathy, occurs after a 2-60 days period of remission which is called the “lucid interval” in about 2-30% patients who recover from acute CO poisoning[2]. Delayed neuropsychologic sequelae refers to symptoms such as impaired memory,

cognitive dysfunction, depression, anxiety, vestibular and motor deficits[3]. At present, hyperbaric oxygen (HBO) therapies is considered as an effective treatment to incidence of DNS[4], but other researchers disputed the effectiveness of HBO therapies[5]. Thus, there is still a lack of effective treatment for delayed neuropsychologic sequelae[6]. The pathogenesis of DNS is complex and not completely clear. It is reported that inflammatory response and oxidative is closely related to the pathophysiological mechanism of CO poisoning[7]; thus, immunomodulatory therapy and antioxidant therapy are essential for patients after CO poisoning[8].

Fasudil, a Rho kinase inhibitor, has been extensively reported to relieve vasospasm in patients with subarachnoid hemorrhage (SAH) by inhibiting the phosphorylation of myosin light chain (MLC)[9, 10]. In addition, several studies revealed that Fasudil has other effects, including anti-inflammatory, anti-apoptosis, reducing oxidative stress and ischemia-reperfusion[11, 12].Fasudil also exert neuroprotective effect and attenuate cognitive function in some neurodegenerative diseases[13]. For example, Kumar et. al[14] reported that Fasudil can alleviate cognitive deficit via inhibiting expression of eNOS and activity of NF-κB mediated by PI3-kianse in STZ-ICV rat model of AD. Huang et. al[15] found that Fasudil can attenuate permeability damage of blood-brain barrier (BBB) and blood-spinal cord barrier (BSCB) in a model of experimental autoimmune encephalomyelitis (EAE). These studies indicated the important role of Fasudil on neuroprotective effect, but it is rarely reported in DNS model, and its potential mechanism has not been clarified. This study focuses on the effect and mechanism of Fasudil in DNS rat model from the perspective of regulating immunity and oxidative stress.

Materials And Methods

Animals

Male Sprague-Dawley (SD) rats weighting 200-250g were obtained from the Experimental Animal Center of Southwest Medical University and placed in a thermostatic specific pathogen-free laboratory animal room with free access to feeds and water. Animal procedures were conducted in accordance with the guidelines of the European Directive 2010/63/EU[16] and was approved by the Ethics Committee of Southwest Medical University (Approval No.20210006).

DNS model

The DNS model was established by hyperbaric oxygen chamber according to published protocol[17]. Briefly rats were exposed to CO (1,000 ppm) for 40 min and then 3,000 ppm for 20 min, until they lost consciousness, and then they were removed to breathe room air and regain consciousness.

Experimental Design and Fasudil administration

In this experiment, DNS model rats were randomly assigned to the CO group, which received intraperitoneal injection of phosphate-buffered saline (PBS), or the CO+FS group, which received intraperitoneal injection of Fasudil. Each group had 10 mice (n=10). And ten mice were exposed to air as

the AC group, which received intraperitoneal injection of PBS. Rats were injected with PBS or fasudil (10 mg/kg) (Sigma Chemical)[18] once daily for 14 consecutive days following model building as shown in Fig.1. Rats were sacrificed for brain tissue collection under deep anesthesia by 10% pentobarbital sodium (40mg/kg)[19].

Morris water maze test (MWM)

The cognitive function of the rats was evaluated by the Morris water maze test as previously described[19]. In the visible platform trial, put a black flag on the platform and release each mouse into the water from one of the four start locations facing the tank wall. Give each mouse 60 s to search for the platform and allow it to stay on it for 10–30 s. Record the time the mouse finds the platform as escape latency, and analyze the swimming speed. Place each mouse into the pool at each of the four different starting quadrants for four trials, moving the platform to a different location with each subsequent trial. In the hidden platform trial, place the same platform without a flag in the SE quadrant. Randomly place the mouse into the pool from each of the four quadrants for four trials and record the escape latency of each trial for subsequent analysis for 5 consecutive days, with the platform and the visual cues at constant positions. If the rats could not find the platform after 2 min, they were pulled onto the platform and the time was recorded as 120 s. In the probe trial, remove the platform and locate each mouse in the NW quadrant, which is the quadrant furthest away from the SE quadrant. Record the time spent in the SW quadrant and the platform crossover number in the maze. The general steps are showed in Fig.1

Luxol fast blue (LFB)

The sections were deparaffinized, rehydrated, and stained with LFB to assess the demyelinated area. Furthermore, white matter demyelination was scored in LFB-stained sections as 1 for normal myelination, 2 for mild or minor demyelination (> 50% myelin staining preserved), or 3 for moderate to severe demyelination (< 50% myelin staining preserved), as reported before[20].

Enzyme-linked immunosorbent assay (ELASA)

The serum levels of tumor necrosis factor (TNF)-α, interleukin (IL)-6, tumor necrosis factor (TGF)-β, methane dicarboxylic aldehyde (MDA), and superoxide dismutase (SOD) activity were determined using a commercial ELISA kit (Affffymetrix Inc., Santa Clara, CA, USA), according to the manufacturer's protocol as reported method[21].

Immunofluorescence analysis

Immunofluorescence staining was carried out as previously described[22]. Brains were isolated and fixed in 4% PFA for 48 h and then dehydrated with a 10% sucrose formaldehyde solution and a 20% sucrose formaldehyde solution for 24 h. Brain tissue at 2 mm thick was cut near the cerebral white matter and was embedded in paraffin. The tissue was then cut into 4-μm-thick continuous brain slices. After dehydration with gradient alcohol and xylene, then reduce endogenous peroxidase activity with 3% H 2 O 2 and blocking with 5% bovine serum for 30 min at room temperature; the tissues were then subsequently

incubated with the primary antibodies for anti-MBP (1:200; BA0094; Boster, USA) at 4 °C overnight. Then, fluorescent dye-conjugated secondary antibody for goat-anti-rabbit (1:50; AS-1110; Aspen, USA) were added for 30 min at 37 °C in the dark. Finally, the nuclei were stained with DAPI solution (1:1000, AS1075; Aspen, USA) for 10 min at room temperature, in darkness. Images were scanned by a Nikon reverse laser-scanning confocal microscope (Nikon, CI-S, Japan). Imaging of the stained sections was photographed using confocal microscopy (Germany). The fluorescence quantitative analysis was performed by ImageJ.

Quantitative Real-Time polymerase chain reaction (QRT-PCR)

Sample collection, RNA isolations and qPCR were carried out as previously described[23]. Total RNA was extracted from cerebral white matter by ExTrizol Reagent (Life Technologies) and then reversed transcribed into cDNA by a cDNA Synthesis Kit (CW2569, Cwbiotech, China) according to the manufacturers' protocols. The primer sequences are designed as following as RhoA forward, TGACACCAGGCGCTAATTCA, RhoA reverse, GCTCTGGCAATGGAGTCTGT; ROCK2 forward, CTGGGAAGAGGCAGCTTCAA, ROCK2 reverse, CTCTGCTGTGGGGTTAAGCA; MLC1 forward, CCAGTCCCATGTTACGGTCC, MLC1 reverse, CTAATCCTGACGCATGGCCT; MYPT1 forward, AGCTGAAGCGCTGGATCG, MYPT1 reverse, CAGGCGGCGAGGAAGAC; GAPDH forward, ACTGTGCCGTTGAATTTGCC, GAPDH reverse, TTGCAGTGGCAAAGTGGAGA. Qt-PCR conditions consisted of an initial denaturing step of 3 min at 95◦C followed by 40 cycles of 3 s denaturation at 95◦C, 20 s annealing at 60◦C, and 20 s extension at 72◦C. Then, the plates were read with a StepOnePlus Real-Time PCR system (4376600, ABI, USA). qPCR was performed with SYBR Green (Biotool, Houston). The mRNA expression was normalized to the mRNA expression of GAPDH, and the results were calculated using the comparative cycle threshold ($\Delta\Delta$Ct) method.

Statistical analysis

All value was analyzed using GraphPad Prism v 7.01. The data were presented as mean ± standard deviation (SD). One-way analysis of variance (ANOVA) followed by LSD multiple-range test or two-way repeated measures analysis of variance (ANOVA) was used to determine the statistical differences. A p-value<0.05 was considered significant.

Results

FS treatment attenuated Spatial Learning and Memory Deficits induced by CO-poisoning

The results of MWM test presented in Figure 2. In the visible platform trial, no significant differences were observed in the escape latency or swimming speed among the groups on the 15th day (Fig.2a, 2b). In the hidden platform trial, the escape latency of three groups all decreased gradually. The escape latency from days 17–20 was longer in the CO group than in the AC group ($p< 0.01$) (Fig.2c), and in the CO+FS group was shorter from days 18–20 than in the AC group ($p< 0.01$) (Fig.2c). In the probe trial, the platform crossover number and the percentage of time in the SW quadrant in the CO group was significantly lower

than in the AC group ($p < 0.01$), whereas a significant reduction of these two parameters were obtained in the CO+FS group in comparison with the CO group ($p < 0.01$) (Fig.2d, 2e). Thus, these results showed that FS attenuated spatial learning and memory deficits induced by CO-poisoning.

FS treatment alleviated the demyelination induced by CO-poisoning

LFB staining and immunofluorescence staining of MBP protein were performed to evaluate demyelination at 21 days post CO-poisoning. As shown in Fig.3a, the LFB staining of white matter from the CO group exhibited irregular vacuoles and broken myelin patches, while this was relatively not obvious in the CO +FS group. Assigning a score to demyelination intensity, CO poisoning significantly increased the demyelination score compared to the AC group ($p <0.05$) (Fig.3b). Furthermore, the lower protein levels of MBP in the CO group also indicated that CO-poisoning could cause evident MBP degradation in the brain tissues ($P< 0.05$) (Fig. 3c, 3d). When Fasudil treatment substantially promoted the remodeling of myelin sheath and alleviated impairment of MBP ($P< 0.05$) (Fig. 3).

FS treatment reduce inflammatory cytokines induced by CO-poisoning

The serum TNF-α, IL-6, and TGF-β levels in the white matter were determined by ELISA on days 21 following CO poisoning. Compared with the AC groups, rats in the CO group exhibited significantly higher levels of TNF-α ($P< 0.01$) (Figure 4a). While the level of IL-6 was slightly increased with no difference ($P>0.05$) (Figure 4b). Treatment with Fasudil significantly decreased the expression of TNF-α and IL-6 ($P< 0.05$) (Figure 4a, 4c). TGF-β levels in the CO group were not significantly different from those in the CO/FS group and AC groups ($P > 0.05$) (Figure 4b). These results indicated that FS could alleviated inflammatory responses on days 21 following CO poisoning.

FS treatment attenuate oxidative stress induced by CO poisoning

To determine the oxidative stress, MDA contents and SOD activity in the hippocampus and white matter were measured. Compared with those in the AC group, the MDA content in the hippocampus and the white matter were obviously increased after CO exposure ($p<0.05$ or $p<0.01$), while FS treatment significantly decreased the production of MDA ($p<0.05$ vs. CO group) (Fig. 5a,5c). The levels of SOD activity were significantly decreased in the hippocampus and the white matter of CO group ($p<0.05$ or $p<0.01$ vs. AC group) (Fig. 5b, 5d). Also, FS administration induced the increase production of SOD ($p<0.05$ vs. CO group). These results indicated that Fasudil could attenuate oxidative stress levels induced by CO poisoning.

Fs treatment inhibit the Rho-Kinase Pathway in DNS rats

Rt-PCR was conducted to measure the expression of Rho, ROCK2, MYPT1 and MLC. Compared with the AC groups, the levels of ROCK2 and MYPT1 mRNA in the CO group were significantly increased after 21 days ($P<0.05$) (Fig.6b, 6d). While the mRNA expression levels of RhoA and MLC were not significantly changed after CO poisoning($P>0.05$) (Fig.6a, 6c). Fasudil treatment significantly lowered the levels of ROCK2, MYPT1, and MLC1 expression ($P<0.01$) (Fig.6b, 6c, 6d) and partially lowered RhoA expression (P>

0.05) (Fig.6a). These results suggest that Fasudil alleviates the RhoA/ROCK-mediated signaling pathway in DNS model.

Discussion

DNS is common in patients after acute CO poisoning[24]. Multiple mechanisms collectively induced disease onset and severity[25]. In the acute stage of carbon monoxide poisoning, the direct toxic effect of CO and its mediated hypoxia leads to mitochondrial dysfunction, oxidative damage, cell apoptosis, activation of inflammatory cascade, demyelination of white matter, immune system dysfunction, especially in organs sensitive to ischemia[26]. It is speculated that MBP was modified by MDA which is ultimate product of membrane lipid peroxidation; thus, MBP lost its normal cationic properties resulting in recognition by an antibody and activating the adaptive immunological response[27, 28]. Therefore, when the progressing injuries of MBP exceed an unknown tripping point, pathophysiological variations in brain tissues and a succession of neurodegenerative symptoms could occur in some patients[29].

The RhoA/ROCK pathway participates in diverse neuronal biological activities, such as migration, dendrite development, and axonal extension[13]. And some studies have confirmed that RhoA / ROCK pathway is related to the pathogenesis of Alzheimer's disease (AD)[30], spinal cord injury (SCI)[31], stroke[32] and experimental autoimmune encephalomyelitis[33]. Rho-associated protein kinase (ROCK) is a downstream effector of RhoA[34], and the most promising drug targets[35]. Fasudil (hexahydro-1-(5-isoquinolylsulfonyl)-1H-1,4-di-azepime), also known as HA-1077, which has the isoquinoline and the homopiperazine ring, is widely used as a ROCK inhibitor[36]. Fasudil has been used in the treatment of neurodegenerative diseases. Study has demonstrated that the learning and memory function of amyloid precursor protein/presenilin-1 transgenic (APP/PS1) mice is significantly enhanced after treatment with Fusudil by modulating gut microbiota and metabolites[37]. Another study about APP/PS1 mice reported that Fasudil increased antioxidative substances, decreased lipid peroxides, and inhibited neuronal apoptosis by inhibiting ROCK/MAPK and activating Nrf2 signaling pathways. Research focusing on the ischemic stroke illustrated that Fasudil combined with bone marrow mesenchymal stem cells (BMSCs) synergistically promotes neurovascular remodeling and neurological function recovery in rat model[38]. In seizure-induced neurite injury, fasudil can increase neurite outgrowth and alleviated spine loss both in Neuro-2a cells and in cultured hippocampal neurons via inhibiting RhoA/Rho kinase pathway[39]. These studies show that fasudil has protective effects on cognition and cerebrovascular function. Therefore, in the current study, we explored the role of Fusudil in delayed encephalopathy after CO poisoning, and the results showed that Fusudil indeed alleviate CO-mediated behavioral disorders and damage of myelin as we expected.

RhoA/ROCK pathway is one of the key regulators of cellular oxidative stress and inflammatory damage[40, 41]. Some studies reported that Rho-kinase (ROCK) inhibitor can downregulate NADPH oxidase 2 (NOX2) expression which promoted by the phosphorylation level of myosin light chain (p-MLC) in rat ischemia/reperfusion (I/R) model[42]. And p-MLC are subjected to MLC kinases, type 1 Ser/Thr phosphatase, and MLC phosphatase (MLCP) activities. The activity of the catalytic subunit of MLCP

depends on its associated regulatory subunit, namely myosin PPase targeting subunit 1 (MYPT1)[43]. Previously published research suggested that chronic stress promotes cognitive impairment and dendritic spine loss in hippocampal neurons possibly by through phosphorylation of the MYPT1 and inactivates MLCP[44]. In addition, researchers found that RhoA/ROCK pathway is an important mediator of the cross-talk between hematopoietic and non-hematopoietic cells which is necessary to efficiently clear pathogens while preventing the emergence of autoimmunity[45]. These results preliminarily elucidated the protective mechanism of RhoA/ROCK pathway. In the study the inflammatory response and oxidative stress increased significantly in DNS model after CO poisoning, as well as the expression of ROCK2 and MYPT1 were markedly increased. In addition, the trend is reversed by treatment of fasudil, which was attributed to the protective effect of fasudil on CO poisoning.

Conclusion

In short, our research shows that Fasudil can alleviate delayed neuropsychologic sequelae by reducing inflammation and oxidative stress mediated by Rho/ROCK2 pathway. This study will provide new ideas for the treatment of CO poisoning.

Abbreviation

Delayed neuropsychologic sequelae (DNS)

carbon monoxide (CO)

Fasudil (FS)

Luxol fast blue (LFB)

myelin basic protein (MBP)

hyperbaric oxygen (HBO)

subarachnoid hemorrhage (SAH)

blood-brain barrier (BBB)

blood-spinal cord barrier (BSCB)

experimental autoimmune encephalomyelitis (EAE)

Sprague-Dawley (SD)

phosphate-buffered saline (PBS)

Morris water maze test (MWM)

Luxol fast blue (LFB)

Enzyme-linked immunosorbent assay (ELASA)

tumor necrosis factor (TNF)-α,

interleukin (IL)-6,

tumor necrosis factor (TGF)-β,

methane dicarboxylic aldehyde (MDA)

superoxide dismutase (SOD)

Quantitative Real-Time polymerase chain reaction (QRT-PCR)

analysis of variance (ANOVA)

Alzheimer's disease (AD)

spinal cord injury (SCI)

Rho-associated protein kinase (ROCK)

Fasudil (hexahydro-1-(5-isoquinolylsulfonyl)-1H-1,4-di-azepime)

bone marrow mesenchymal stem cells (BMSCs)

NADPH oxidase 2 (NOX2)

ischemia/reperfusion (I/R)

myosin light chain (MLC)

MLC phosphatase (MLCP)

myosin PPase targeting subunit 1 (MYPT1)

Declarations

Ethics approval and consent to participate

Animal procedures were conducted in accordance with the guidelines of the European Directive 2010/63/EU and was approved by the Ethics Committee of Southwest Medical University (Approval No.20210006). This study was carried out in compliance with ARRIVE guidelines.

Consent for publication

Not applicable.

Availability of data and materials

All data generated or analysed during the current study are included in this published article.

Competing interests

The authors declare that they have no competing interests.

Funding

This study was financially supported by the Luzhou People's Government-Southwest Medical University science and technology strategic cooperation project (Grant No.2017LZXNYD-J36).

Authors' contributions

YX and LJ designed the work, and wrote the manuscript. YX, FM, LS, XH, GY, and HQ assisted to performed the experiments and analyzed the data. All authors have reviewed and approved the final version of the manuscript, and agree to be accountable for all aspects of the work.

Acknowledgements

Not applicable.

References

1. Garg J, Krishnamoorthy P, Palaniswamy C, Khera S, Ahmad H, Jain D, Aronow WS, Frishman WH. Cardiovascular Abnormalities in Carbon Monoxide Poisoning. Am J Ther 2018, 25(3):e339-e348.
2. Guo D, Hu H, Pan S. Oligodendrocyte dysfunction and regeneration failure: A novel hypothesis of delayed encephalopathy after carbon monoxide poisoning. Med Hypotheses 2020, 136:109522.
3. Ning K, Zhou YY, Zhang N, Sun XJ, Liu WW, Han CH. Neurocognitive sequelae after carbon monoxide poisoning and hyperbaric oxygen therapy. Med Gas Res 2020, 10(1):30-36.
4. Kim SJ, Thom SR, Kim H, Hwang SO, Lee Y, Park EJ, Lee SJ, Cha YS. Effects of Adjunctive Therapeutic Hypothermia Combined With Hyperbaric Oxygen Therapy in Acute Severe Carbon Monoxide Poisoning. Crit Care Med 2020, 48(8):e706-e714.
5. Kitamoto T, Tsuda M, Kato M, Saito F, Kamijo Y, Kinoshita T. Risk factors for the delayed onset of neuropsychologic sequelae following carbon monoxide poisoning. Acute Med Surg 2016, 3(4):315-319.
6. Kudo K, Otsuka K, Yagi J, Sanjo K, Koizumi N, Koeda A, Umetsu MY, Yoshioka Y, Mizugai A, Mita T *et al*. Predictors for delayed encephalopathy following acute carbon monoxide poisoning. BMC Emerg Med 2014, 14:3.

7. Zhang J, Wu H, Zhao Y, Zu H. Therapeutic Effects of Hydrogen Sulfide in Treating Delayed Encephalopathy After Acute Carbon Monoxide Poisoning. Am J Ther 2016, 23(6):e1709-e1714.
8. Teksam O, Sabuncuoğlu S, Girgin G, Özgüneş H. Evaluation of oxidative stress and antioxidant parameters in children with carbon monoxide poisoning. Hum Exp Toxicol 2019, 38(11):1235-1243.
9. Zhao JZ, Zhou DB, Guo J, Ren ZY, Zhou LF, Wang S, Zhang Y, Xu BN, Zhao KM, Wang RZ *et al*. Efficacy and Safety of Fasudil in Patients With Subarachnoid Hemorrhage: Final Results of a Randomized Trial of Fasudil Versus Nimodipine. Neurologia Medico-Chirurgica 2011, 51(10):679-683.
10. Tsounapi P, Saito M, Kitatani K, Dimitriadis F, Ohmasa F, Shimizu S, Kinoshita Y, Takenaka A, Satoh K. Fasudil improves the endothelial dysfunction in the aorta of spontaneously hypertensive rats. European Journal of Pharmacology 2012, 691(1-3):182-189.
11. Iyer M, Subramaniam MD, Venkatesan D, Cho SG, Ryding M, Meyer M, Vellingiri B. Role of RhoA-ROCK signaling in Parkinson's disease. Eur J Pharmacol 2021, 894:173815.
12. Yanagida Y, Namba M, Fukuta T, Yamamoto H, Yanagida M, Honda M, Oku N, Asai T. Release rate is a key variable affecting the therapeutic effectiveness of liposomal fasudil for the treatment of cerebral ischemia/reperfusion injury. Biochem Biophys Res Commun 2020, 531(4):622-627.
13. Fujita Y, Yamashita T. Axon growth inhibition by RhoA/ROCK in the central nervous system. Front Neurosci 2014, 8:338.
14. Kumar M, Bansal N. Fasudil hydrochloride ameliorates memory deficits in rat model of streptozotocin-induced Alzheimer's disease: Involvement of PI3-kinase, eNOS and NF kappa B. Behavioural Brain Research 2018, 351:4-16.
15. Huang XN, Fu J, Wang WZ. The effects of fasudil on the permeability of the rat blood-brain barrier and blood-spinal cord barrier following experimental autoimmune encephalomyelitis. Journal of neuroimmunology 2011, 239(1-2):61-67.
16. De Sio F, Hanke FD, Warnke K, Marazia C, Galligioni V, Fiorito G, Stravidou I, Ponte G. E Pluribus Octo - Building Consensus on Standards of Care and Experimentation in Cephalopod Research; a Historical Outlook. Frontiers in Physiology 2020, 11.
17. Fan DF, Hu HJ, Sun Q, Lv Y, Ye ZH, Sun XJ, Pan SY. Neuroprotective effects of exogenous methane in a rat model of acute carbon monoxide poisoning. Brain Res 2016, 1633:62-72.
18. Kim J, Joshi HP, Kim KT, Kim YY, Yeo K, Choi H, Kim YW, Choi UY, Kumar H, Sohn S *et al*. Combined Treatment with Fasudil and Menthol Improves Functional Recovery in Rat Spinal Cord Injury Model. Biomedicines 2020, 8(8).
19. Ji E, Wang J, Wang L, Pan Z, Gao W. Pharmacological Effects of Fasudil on Flap Survival in a Rodent Model. J Surg Res 2020, 255:575-582.
20. Kafami L, Etesami I, Felfeli M, Enayati N, Ghiaghi R, Aminian A, Dehpour A. Methadone diminishes neuroinflammation and disease severity in EAE through modulating T cell function. Journal of neuroimmunology 2013, 255(1-2):39-44.

21. Wang X, Zhao B, Li X. Dexmedetomidine attenuates isoflurane-induced cognitive impairment through antioxidant, anti-inflammatory and anti-apoptosis in aging rat. International journal of clinical and experimental medicine 2015, 8(10):17281-17288.
22. Xu W, Yan J, Chen S, Ocak U, Shao A, Zhang J. Peroxisomal Dysfunction Contributes to White Matter Injury Following Subarachnoid Hemorrhage in Rats via Thioredoxin-Interacting Protein-Dependent Manner. Frontiers in cell and developmental biology 2020, 8:576482.
23. Yin Y, Qin Z, Xu X, Liu X, Zou H, Wu X, Cao J. Inhibition of miR-124 improves neonatal necrotizing enterocolitis via an MYPT1 and TLR9 signal regulation mechanism. Journal of cellular physiology 2019, 234(7):10218-10224.
24. Choi S, Han S, Nah S, Lee YH, Cho YS, Lim H, Kim MS, Kim GW. Effect of ethanol in carbon monoxide poisoning and delayed neurologic sequelae: A prospective observational study. PLoS One 2021, 16(1):e0245265.
25. Xiang WP, Xue H, Wang BJ. Delayed encephalopathy of acute carbon monoxide intoxication in rats: potential mechanism and intervention of dexamethasone. Pakistan Journal of Pharmaceutical Sciences 2014, 27(6):2025-2028.
26. Yang CC, Chuang YF, Chen PE, Tao P, Tung TH, Chien CW. The occurrence of delayed neuropsychologic sequelae in acute carbon monoxide poisoning patients after treatment with hyperbaric or normobaric oxygen therapy. Medicine (Baltimore) 2021, 100(2):e24183.
27. Zhang J, Sun X, Zheng S, Liu X, Jin J, Ren Y, Luo J. Myelin basic protein induces neuron-specific toxicity by directly damaging the neuronal plasma membrane. PLoS One 2014, 9(9):e108646.
28. Xiang WP, Xue H, Wang BJ. Delayed encephalopathy of acute carbon monoxide intoxication in rats: potential mechanism and intervention of dexamethasone. Pak J Pharm Sci 2014, 27(6 Suppl):2025-2028.
29. Thom SR, Bhopale VM, Fisher D, Zhang J, Gimotty P. Delayed neuropathology after carbon monoxide poisoning is immune-mediated. Proc Natl Acad Sci U S A 2004, 101(37):13660-13665.
30. Cai R, Wang Y, Huang Z, Zou Q, Pu Y, Yu C, Cai Z. Role of RhoA/ROCK signaling in Alzheimer's disease. Behav Brain Res 2021, 414:113481.
31. Wu X, Xu XM. RhoA/Rho kinase in spinal cord injury. Neural Regen Res 2016, 11(1):23-27.
32. Lu W, Chen Z, Wen J. RhoA/ROCK signaling pathway and astrocytes in ischemic stroke. Metab Brain Dis 2021, 36(6):1101-1108.
33. Yan Y, Yu J, Gao Y, Kumar G, Guo M, Zhao Y, Fang Q, Zhang H, Yu J, Jiang Y *et al*. Therapeutic potentials of the Rho kinase inhibitor Fasudil in experimental autoimmune encephalomyelitis and the related mechanisms. Metab Brain Dis 2019, 34(2):377-384.
34. Chuang HH, Yang CH, Tsay YG, Hsu CY, Tseng LM, Chang ZF, Lee HH. ROCKII Ser(1366) phosphorylation reflects the activation status. Biochemical Journal 2012, 443:145-151.
35. Tönges L, Koch JC, Bähr M, Lingor P. ROCKing Regeneration: Rho Kinase Inhibition as Molecular Target for Neurorestoration. Front Mol Neurosci 2011, 4:39.

36. Carneiro A, De Vito FB, Moraes-Souza H, Crema VO. RhoA/ROCKs signaling is increased by treatment with TKI-258 and leads to increased apoptosis in SCC-4 oral squamous cell carcinoma cell line. J Oral Pathol Med 2021, 50(4):394-402.
37. Yan Y, Gao Y, Fang Q, Zhang N, Kumar G, Yan H, Song L, Li J, Zhang Y, Sun J *et al*. Inhibition of Rho Kinase by Fasudil Ameliorates Cognition Impairment in APP/PS1 Transgenic Mice via Modulation of Gut Microbiota and Metabolites. Front Aging Neurosci 2021, 13:755164.
38. Wang Q, Zhao SF, Xiao X, Liu YN, Wang XL, Du YX. Combined Treatment of Bone Marrow Mesenchymal Stem Cells and Fasudil Promotes Neurovascular Remodeling and Neurological Function Recovery in Ischemic Stroke. Applied Biochemistry and Biotechnology.
39. Quadir H, Hakobyan K, Gaddam M, Ojinnaka U, Ahmed Z, Kannan A, Mostafa JA. Role of Rho-Associated Protein Kinase Inhibition As Therapeutic Strategy for Parkinson's Disease: Dopaminergic Survival and Enhanced Mitophagy. Cureus 2021, 13(8):e16973.
40. Liang J, Zeng X, Halifu Y, Chen W, Hu F, Wang P, Zhang H, Kang X. Blocking RhoA/ROCK inhibits the pathogenesis of pemphigus vulgaris by suppressing oxidative stress and apoptosis through TAK1/NOD2-mediated NF-κB pathway. Mol Cell Biochem 2017, 436(1-2):151-158.
41. Tiftik RN, Temiz-Reşitoğlu M, Güden DS, Bayrak G, Ün İ, Yılmaz Ş N, Şahan-Fırat S. Involvement of Rho-kinase/IκB-α/NF-κB activation in IL-1β-induced inflammatory response and oxidative stress in human chondrocytes. Can J Physiol Pharmacol 2021, 99(4):418-426.
42. Zhang YS, Tang LJ, Tu H, Wang SJ, Liu B, Zhang XJ, Li NS, Luo XJ, Peng J. Fasudil ameliorates the ischemia/reperfusion oxidative injury in rat hearts through suppression of myosin regulatory light chain/NADPH oxidase 2 pathway. Eur J Pharmacol 2018, 822:1-12.
43. Kim KM, Csortos C, Czikora I, Fulton D, Umapathy NS, Olah G, Verin AD. Molecular characterization of myosin phosphatase in endothelium. Journal of cellular physiology 2012, 227(4):1701-1708.
44. Castañeda P, Muñoz M, García-Rojo G, Ulloa JL, Bravo JA, Márquez R, García-Pérez MA, Arancibia D, Araneda K, Rojas PS *et al*. Association of N-cadherin levels and downstream effectors of Rho GTPases with dendritic spine loss induced by chronic stress in rat hippocampal neurons. J Neurosci Res 2015, 93(10):1476-1491.
45. Ricker E, Chowdhury L, Yi W, Pernis AB. The RhoA-ROCK pathway in the regulation of T and B cell responses. F1000Res 2016, 5.

Tables

Table1

RhoA	Forward primer	TGACACCAGGCGCTAATTCA
	Reverse primer	GCTCTGGCAATGGAGTCTGT
Rock2	Forward primer	CTGGGAAGAGGCAGCTTCAA
	Reverse primer	CTCTGCTGTGGGGTTAAGCA
Mlc1	Forward primer	CCAGTCCCATGTTACGGTCC
	Reverse primer	CTAATCCTGACGCATGGCCT
Mypt1	Forward primer	AGCTGAAGCGCTGGATCG
	Reverse primer	CAGGCGGCGAGGAAGAC
GAPDH	Forward primer	ACTGTGCCGTTGAATTTGCC
	Reverse primer	TTGCAGTGGCAAAGTGGAGA

Figures

Figure1

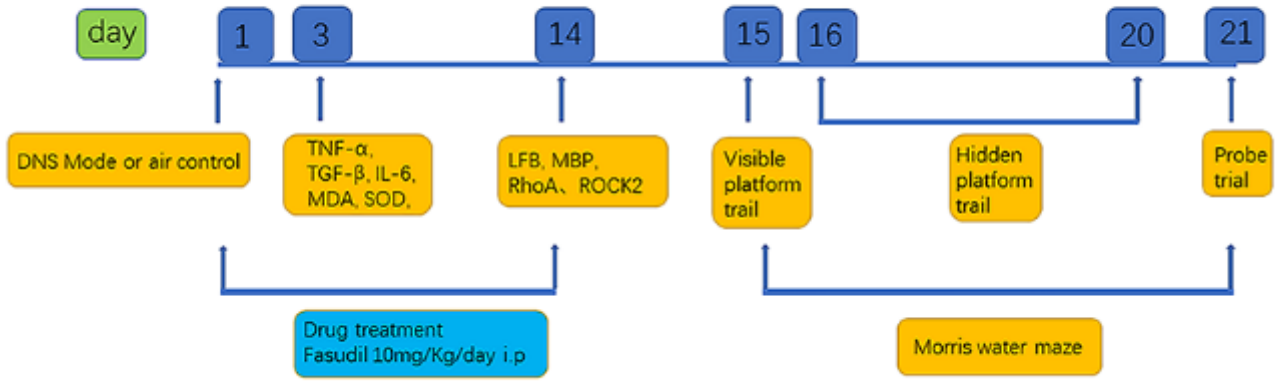

Figure 1

Flow diagram of this study. DNS, delayed neuropsychologic sequelae; LFB, luxol fast blue; MBP, myelin basic protein; TNF-α, rat tumor necrosis factor-α; TGF-β, tumor necrosis factor-β; IL-6, interleukin-6; MDA, Malondialdehyde; RhoA, ras homolog family member A; ROCK2, Rho-associated protein kinases.

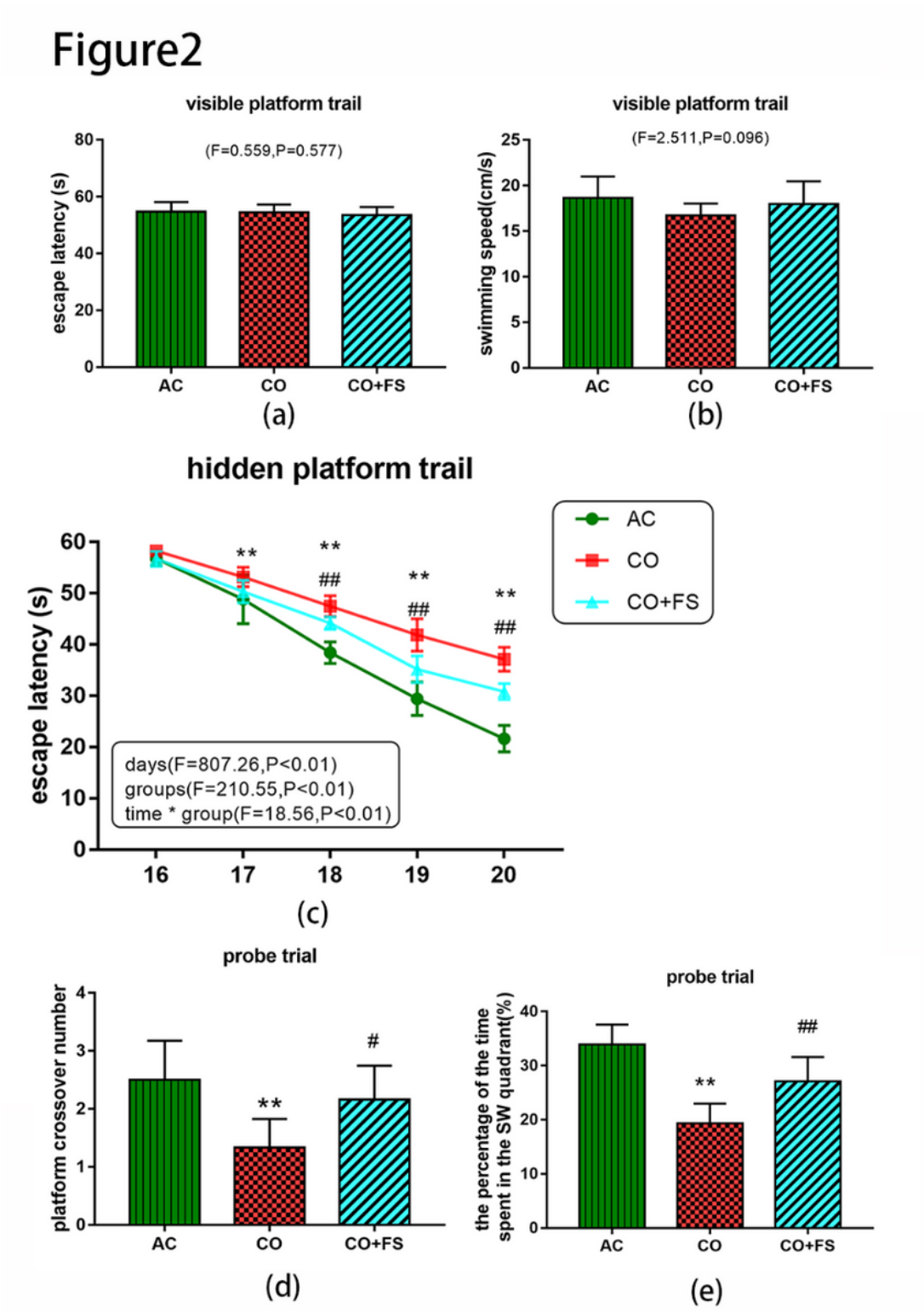

Figure 2

FS attenuated Spatial Learning and Memory Deficits induced by CO-poisoning. In the visible platform trial, the escape latency (a) and swimming speed (b) of rats in the AC, CO, and CP+FS group. (c) Changes in the escape latency of rats among the three groups in the hidden platform trials. In the probe trial, the platform crossover number (d) and the percentage of the time spent in the SW quadrant (e) among the different groups. The results of each group are shown as mean ± SD (n=10). The symbol * indicates

p<0.05 and ** indicates p<0.01 vs. the AC group; # indicates p<0.05 and ## indicates p<0.01 vs. the CO group.

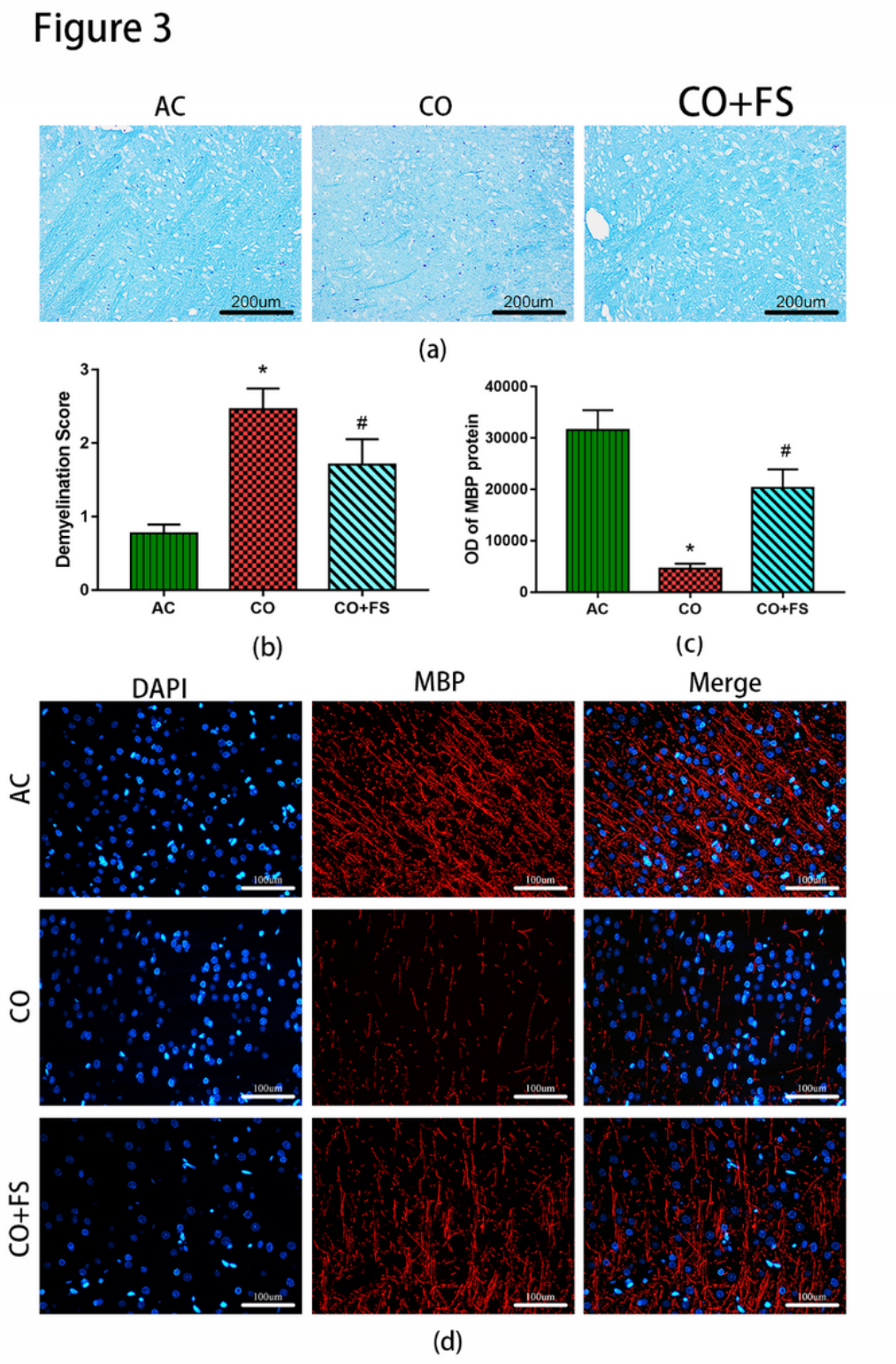

Figure 3

FS alleviated the demyelination induced by CO-poisoning. (a) Luxol fast blue (LFB) and (b) demyelination score of brain sections from rats in the AC, CO, CO+FS group, Scale bar =200 μm. (d) Immunofluorescence images and (c) quantification showed the expression of MBP (red) and nuclear

(blue) in the AC, CO, CO+FS groups, Scale bar =100 μm. The data in each group are shown as mean ± SD (n=10). The symbol * indicates p< 0.05 vs.AC group and # indicates p<0.05 vs. the CO group.

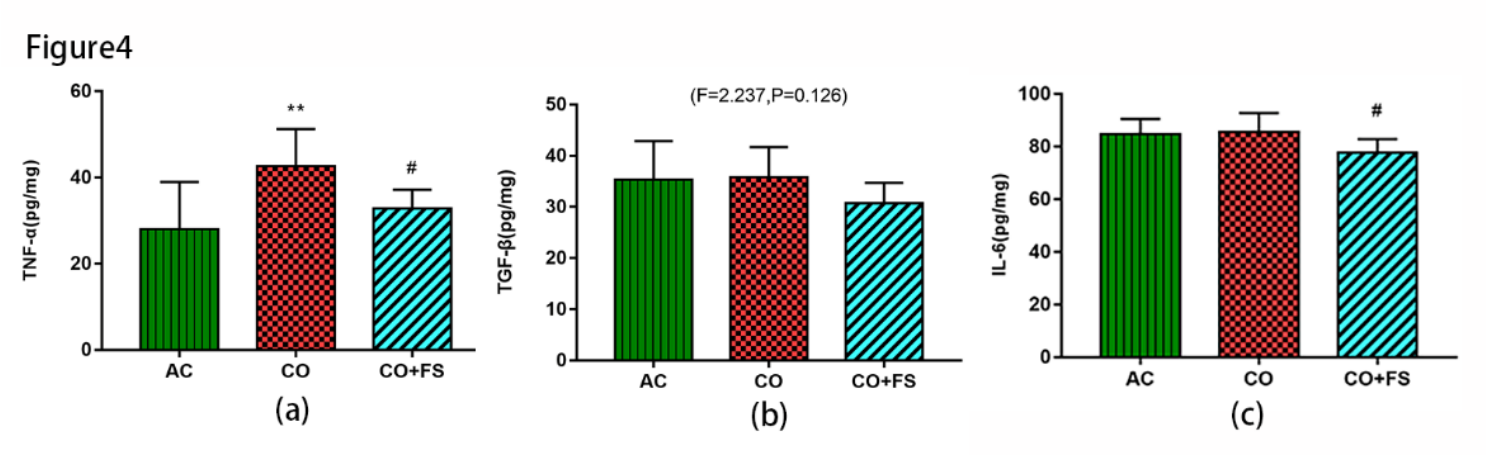

Figure 4

FS reduce inflammatory cytokines induced by CO-poisoning. The serum levels of (a) TNF-α, (b)TGF-β, and (c) IL-6 were assayed by ELASA. The data in each group are shown as mean ± SD (n=10). The symbol ** indicates p<0.01 vs. AC group and ## indicates p<0.01 vs. the CO group. ELISA: enzyme-linked immunosorbent assay. TNF-α, tumor necrosis factor-α; TGF-β: tumor necrosis factor-β; IL-6, interleukin 6.

Figure5

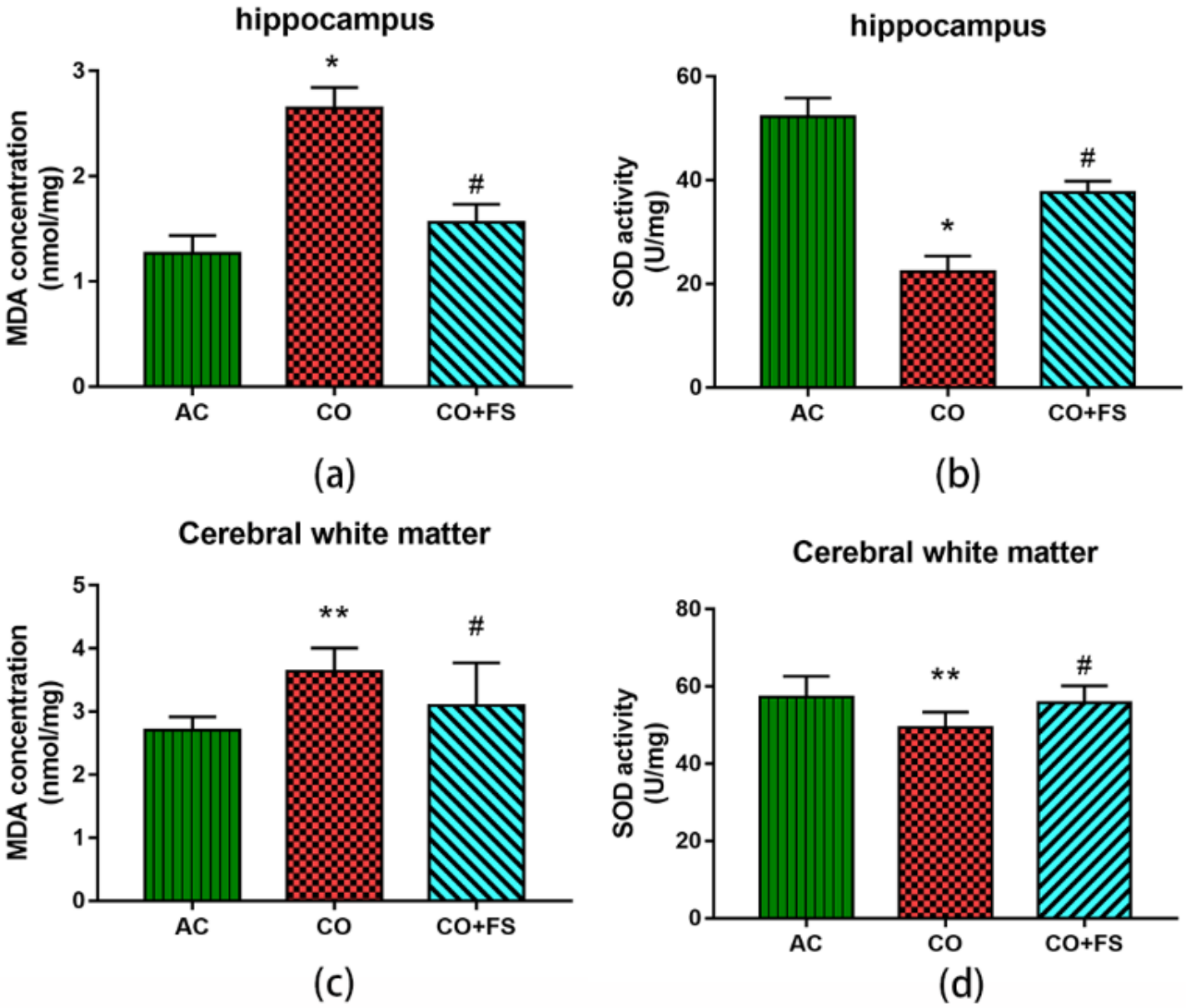

Figure 5

FS inhibited oxidative injury induced by CO poisoning. On postexposure day 21, we collected hippocampus tissue and cerebral white matter in different groups and measured the concentration of MDA (a, c) and activity of SOD (b, d). The data in each group are shown as mean ± SD (n=10). The symbol * indicates $p<0.05$ and ** indicates $p<0.01$ vs.AC group; # indicates $p<0.05$ vs. the CO group. MDA, Malondialdehyde; SOD, Superoxide dismutase.

Figure6

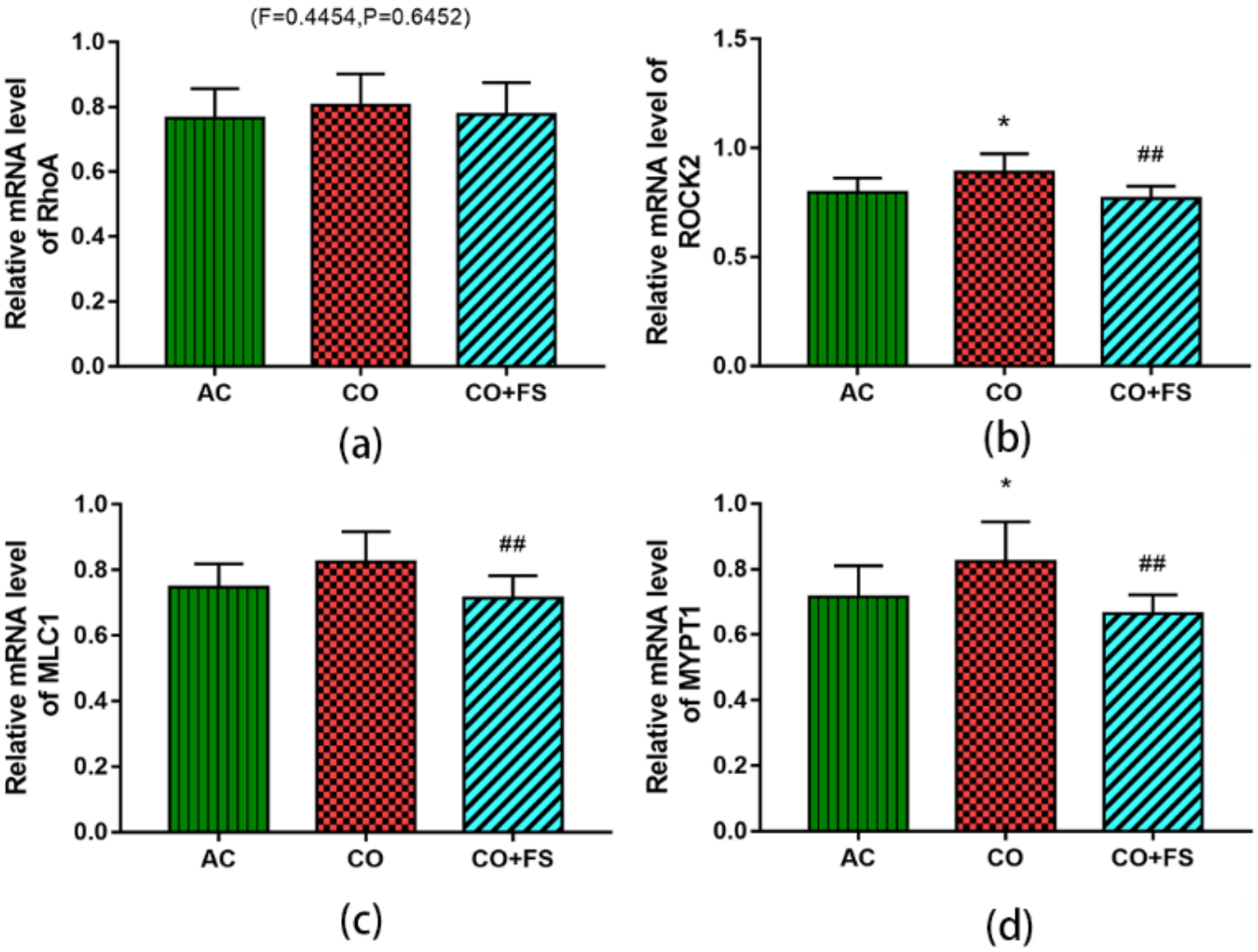

Figure 6

FS attenuated the RhoA/ROCK-mediated pathway in DNS. The mRNA levels of RhoA□a□, ROCK2 (b), MLC (c), and MYPT1 (d) in the CA1 region of the hippocampus by real-time PCR. Data are expressed as the mean ± SD, n=10. The symbol * indicates $p<0.05$ vs.AC group; ## indicates $p<0.01$ vs. the CO group.